Effect of Deuterium Substitution on Electron Transfer at Cytochrome *c*/SAM Interfaces

Kathryn L. Davis and David H. Waldeck*

Department of Chemistry, University of Pittsburgh, Pittsburgh, Pennsylvania 15260

Received: April 7, 2008; Revised Manuscript Received: July 24, 2008

The involvement of protons in the heterogeneous electron transfer between cytochrome *c* and a gold electrode to which it is attached was studied by comparing the electron transfer rate constants for H_2O and D_2O solutions. Rate constants were measured as a function of the electrochemical cell solution and the protein incubant solution, i.e., k^0(incubant, cell). Two separate isotope effects exist: a cell "isotope effect", $KIE_{cell} = k^0(H_2O, H_2O):k^0(H_2O, D_2O)$, which is manifest at short time scales (<30 s) and arises from the viscosity difference between H_2O and D_2O, and an incubant isotope effect, $KIE_{inc} = k^0(H_2O, H_2O):k^0(D_2O, H_2O)$, which is manifest at longer times (>2 h) and results from H/D exchange. The two isotope effects are approximately equal (~1.2) and a total isotope effect $KIE_{total} = k^0(H_2O, H_2O):k^0(D_2O, D_2O)$ can be constructed that is the product of KIE_{cell} and KIE_{inc}. The nature of the electron transfer process, possible coupling to a proton transfer process, and the involvement of specific hydrogens in the transfer mechanism are discussed.

Introduction

Cytochrome *c* is a redox-active protein that plays an important role in cell respiration. Because it is small (104 residues, MW ca. 12 kDa), easily purified and is accessible to spectroscopic probes, it has been extensively studied in past decades, both to understand its own structure and function and as a model of more complex proteins. Despite many studies, however, the electron transfer mechanism is still not completely understood.

Chemically modified silver and gold electrode surfaces have been useful in studies intended to clarify the electron transfer mechanism of cytochrome *c*. By forming self-assembled alkanethiol monolayers (SAMs) of varying length and terminal group composition, a variety of electron transfer complex compositions and orientations can be accessed.[1−17] For example, adsorption to a pure $-S(CH_2)_mCOOH$ or mixed $-S(CH_2)_mCOOH/-S(CH_2)_nOH$ SAM via electrostatic interactions between cationic lysine residues on the protein and anionic carboxylate residues on the SAM (Figure 1A) results in a situation that is similar to the interaction of cytochrome *c* with cytochrome *c* oxidase,[18] its biological electron transfer partner. Electrostatic interactions can be converted to amide bonds using a covalent cross-linking reagent such as EDC[19,20] or CMC,[17,21,22] as illustrated by Figure 1B, leading to an electron transfer complex in which large-scale rotational motion of the protein is restricted. Another binding motif (not shown) is also possible,[6,16,17,22,23] in which the protein surface-SAM interaction is bypassed entirely by using a pyridine-terminated alkanethiol to directly ligate the heme iron.

The electron transfer rate constant exhibits an interesting dependence on SAM thickness, which reflects a change of the rate-limiting process in the electron transfer mechanism. For thick SAMs, an exponential distance dependence, which is characteristic of electron transfer that is controlled by electron tunneling, is observed. At shorter chain lengths, however, the electron transfer rate increases only weakly with decreasing distance; this is sometimes referred to as the plateau region. This type of distance dependence has been reported for electrostatically adsorbed,[1,7] covalently attached[21] and pyridine-ligated[6,14,16] cytochrome *c* assemblies, as well as for azurin immobilized on gold electrodes,[25,26] for ferrocene and ruthenium redox couples tethered to alkanethiol or oligophenyleneethylene monolayers on gold,[27−29] and for ferri/ferrocyanide diffusing to gold electrodes coated with alkanethiol monolayers of varying length.[30] Several hypotheses have been proposed to explain the rate-limiting process in the plateau region, including conformational gating,[1] proton-coupled electron transfer affected by the applied electric field,[7] and electron transfer limited by polarization relaxation processes of the protein and the medium.[6]

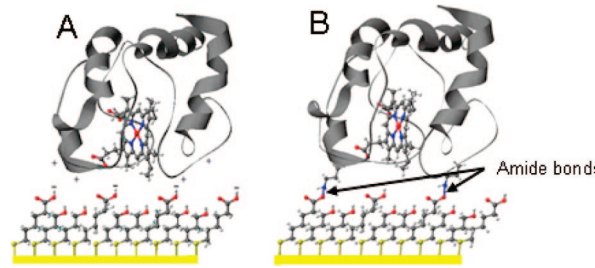

Figure 1. Cartoons representing the two cytochrome *c* binding modes used in this study. Panel A: cytochrome *c* is adsorbed to the carboxylate moieties on a mixed 2:3 $-S(CH_2)_5COOH/-S(CH_2)_4OH$ SAM via electrostatic interactions between lysine residues and carboxylate groups. Panel B: cytochrome *c* is tethered to the same monolayer as in A via two covalent bonds between lysine residues and terminal carboxylate groups. More than two bonds are possible; see ref 24.

An evaluation of the kinetic isotope effect is important to understanding the nature of the rate-limiting process in the plateau region. Several evaluations of the isotope effect for cytochrome *c* immobilized on SAMs of varying length and terminal composition have been reported in the literature. Murgida and Hildebrandt observed a kinetic isotope effect for cytochrome *c* electrostatically adsorbed to pure carboxyl-terminated SAMs having six or fewer methylene groups; it increased with decreasing film thickness from 1.2 at a $-S(CH_2)_5COOH$ SAM to 4.0 at a $-SCH_2COOH$ SAM.[7] For a cytochrome *c* pyridine-ligated to a $-S(CH_2)_{11}Py/-S(CH_2)_9CH_3$ SAM (plateau regime), Khoshtariya et al.[6] report that the rate decreases by ~30% when the protein is exposed to D_2O for 30

* Corresponding author. E-mail: dave@pitt.edu.

10.1021/jp803006b CCC: $40.75
Published on Web 09/09/2008

min or more, while brief exposure results in no change in the rate. In contrast, no isotope effect was observed at $-S(CH_2)_{16}Py/-S(CH_2)_{14}CH_3$ SAMs (tunneling regime). Most recently, Kang et al.[5] used transient absorption spectroscopy to study single crystal zinc cytochrome *c* porphyrin:yeast cytochrome *c* complexes and electrochemical studies of yeast cytochrome *c* electrostatically adsorbed to $-S(CH_2)_{10}COOH/-S(CH_2)_6OH$ SAMs to probe solvent isotope effects. For H_2O-incubated films and crystals, they found an initial rate increase upon exposure to D_2O that was followed by a prolonged decrease in the rate constant up to 72 h after exposure. In general, a KIE of unity is observed at long distances, while the KIE is greater than one in the plateau region.

The purpose of this study is to clarify further the nature of the kinetic isotope effect observed in electrostatic assemblies by Murgida and Hildebrandt and Kang et al. by extending such work to covalent assemblies, for which the kinetic isotope effect has not been reported. Of particular interest is the dissection of the isotope effect into two parts: one caused by immediate changes in the cell solvent and a second caused by prolonged exposure to D_2O, referred to as cell and incubant isotope effects, respectively. These effects were examined by preparing electrostatic and covalent assemblies in either H_2O or D_2O incubant buffer and then transferring them into an electrochemical cell composed of either H_2O or D_2O buffer. The standard electrochemical rate constant, k^0, was determined for the four possible cell/incubant solution permutations. For convenience, it is reported as a function of the incubant and cell isotopes; that is, the rate constant k^0(incubant, cell) measured for H_2O-incubated protein in H_2O solution will be referred to as $k^0(H_2O, H_2O)$, that for the D_2O-incubated protein in H_2O solution will be referred to as $k^0(D_2O, H_2O)$, and so on.

The presence of a deuterium isotope effect was tested for both the tunneling and plateau regions. A kinetic isotope effect of unity was observed for long-chain electrostatic and covalent cytochrome *c*/SAM assemblies, indicating that hydrogen exchange has no effect on electron transfer kinetics in the tunneling region. For short-chain assemblies, two separate isotope effects were observed: a cell 'isotope effect,' $KIE_{cell} = k^0(H_2O, H_2O):k^0(H_2O, D_2O)$, that is manifest at short time scales (<30 s) and arises from the viscosity difference between H_2O and D_2O, and an incubant isotope effect, $KIE_{inc} = k^0(H_2O, H_2O):k^0(D_2O, H_2O)$, manifest at long time scales (>2 h) and resulting from H-D exchange. The two isotope effects are approximately equal and a total isotope effect $KIE_{total} = k^0(H_2O, H_2O):k^0(D_2O, D_2O)$ can be constructed that is the product of KIE_{cell} and KIE_{inc}. These results show that the change in rate constant upon change from H_2O to D_2O has two contributions, one associated with the solvent viscosity and one associated with H/D exchange in the protein matrix.

Experimental Section

Electrode Preparation. Gold wire (0.5 mm diameter, 99.995%) was refluxed in concentrated nitric acid for 30−60 min, then rinsed with deionized water. The tip of the wire was heated in a flame to form a ball of ~0.1 mm diameter with an average area of ~0.09 cm^2 as characterized by cyclic voltammetery in a 0.5 M KCl solution containing 1 mM $K_3[Fe(CN)_6]$ and 1 mM $K_4[Fe(CN)_6]$. A smooth surface was obtained by annealing the ball 10−20 times. The rest of the wire was then sealed in a glass capillary tube. The electrodes were then placed into an alkanethiol solution in ethanol for at least 12 h. Thiol solutions were either 0.8 mM $HS(CH_2)_{10}COOH$/1.2 mM $HS(CH_2)_8OH$ or 0.8 mM $HS(CH_2)_5COOH$/1.2 mM $HS(CH_2)_4OH$. After the electrodes were removed from the thiol solution, they were rinsed thoroughly, first in ethanol, and then in deionized water to prepare for the attachment of cytochrome *c*.

Electrostatic Adsorption. Rinsed electrodes were submerged in 40 μL of cytochrome *c* solution (30−40 μM) in 4.4 mM, pH 8.0 potassium phosphate buffer solution for 30−60 min. Before being placed into the electrochemical cell, electrostatic assemblies were rinsed with 4.4 mM, pH 8.0 phosphate buffer to remove physisorbed and/or weakly bound cytochrome *c* from the surface. Note that a rinse with a buffer solution of pH = 7 gives the same results as the pH = 8 buffer.

Covalent Attachment. Rinsed electrodes were first placed into a solution of the cross-linking reagent *N*-Cyclohexyl-*N*′-(2-morpholinoethyl)carbodiimide methyl-*p*-toluenesulfonate (CMC) in 200 mM pH 7 potassium phosphate buffer in H_2O (I = 400 mM, 20 mg CMC/10 mL buffer) for 30 min. They were then transferred to 40 μL of cytochrome *c* solution (30−40 μM) in 4.4 mM, pH 8 potassium phosphate buffer in H_2O for 30−60 min. Electrodes were rinsed with 200 mM, pH 7 phosphate buffer (I = 400 mM) before being placed in the electrochemical cell. A higher ionic strength rinse solution was used for covalent assemblies because it ensures that only covalently attached cytochrome *c* is under study, see ref 21 for more details.

Electrochemical Measurements. Cyclic voltammetry (CV) was performed using a CH Instruments 618B or CHI430 electrochemical analyzer. The three-electrode cell contained a Ag/AgCl (1 M KCl) reference electrode, a platinum wire counter electrode and a chemically modified gold wire electrode. Voltammetry measurements were made in 80 mM, pH 7 potassium phosphate buffer (I = 160 mM) in H_2O or D_2O (henceforth referred to as the cell solution). At this ionic strength, all weakly bound cytochrome *c* has been desorbed from the surface, and only the most strongly bound cytochrome *c*/SAM complexes remain, which have been shown to have a more favorable electron transfer geometry.[17] The rate constants measured for cytochrome *c*/SAM assemblies at this ionic strength were reproducible and the voltammetry was nearly ideal (*vide infra*), indicating that the electron transfer complexes under study are stable under these experimental conditions. Voltammograms were collected at increasing scan rates from 0.01 to 1000 V/s. Kinetic information was obtained by plotting the separation of the peaks in the voltammogram against the scan rate and then fitting the data to a curve based on Marcus theory.[31,32] The reorganization energy, λ, was chosen to be 0.6 eV per earlier electrochemical studies made in this laboratory;[13] the rate constants determined using this value were not changed by varying λ by ±0.2 eV. Note that any changes in the value of λ would systematically change all of measured k^0 values reported herein; the trends and observed isotope effects would remain the same.

Isotope Studies. Experiments in which cytochrome *c* was either incubated in D_2O buffer or transferred to D_2O solution after incubation in H_2O buffer were performed to probe the nature of the isotope effect on electron transfer. Either electrostatic or covalent cytochrome *c*/SAM assemblies were prepared from cytochrome *c* dissolved in H_2O (H_2O-incubated) or in D_2O (D_2O-incubated) buffer. An initial voltammogram set was collected in phosphate buffer that matched the incubant solvent. From this point, two different types of experiments could be performed. The first type was intended to observe the isotope effect on a short time scale. It consisted of collecting a voltammogram set in a buffer of the opposite isotope (referred to as the countersolvent), followed by a second voltammogram

TABLE 1: Voltammetric Properties of Cytochrome *c*/SAM Assemblies[a]

attachment method		H_2O incubant			D_2O incubant		
		ΔE_p (mV)[d]	$E^{0\prime}$ (mV)	fwhm (mV)[d]	ΔE_p (mV)	$E^{0\prime}$ (mV)	fwhm (mV)[b]
electrostatic	short chain[b]	17 ± 12	0 ± 12	110 ± 11	22 ± 5	0 ± 8	113 ± 5
	long chain[c]	17 ± 15	1 ± 11	108 ± 12	23 ± 10	7 ± 5	104 ± 8
covalent	short chain	17 ± 15	6 ± 6	95 ± 9	16 ± 5	1 ± 16	104 ± 11
	long chain	21 ± 6	2 ± 8	99 ± 3	16 ± 9	8 ± 4	98 ± 10

[a] In the determination of ΔE and fwhm values, a small number of scans (1−2 for electrostatic systems, 4−5 for covalent systems) were discarded from the data set, as the fit by the Marcus model was poor at the lowest scan rates, but acceptable at higher rates. [b] Corresponds to $-S(CH_2)_5COOH/-S(CH_2)_4OH$ SAMs. [c] Corresponds to $-S(CH_2)_{10}COOH/-S(CH_2)_8OH$ SAMs. [d] Reported at 10 V/s for short-chain assemblies and at 1 V/s for long-chain assemblies.

set in the incubant solvent, and a final set in the countersolvent. The two countersolvent studies are referred to as Scan Series 1 and Scan Series 2. The second type of experiment examined the long-term effect of isotopic exchange on electron transfer. In this experiment, the electrode was transferred to the countersolvent and allowed to remain there for up to two hours. A voltammogram set was then collected every ten minutes for the first hour and every thirty minutes during the second hour. In the case of electrostatic systems, the cell potential was held at +0.3 V between voltammogram sets to prevent cytochrome *c* desorption. In order to better ensure the isotopic purity of D_2O, all D_2O solutions were prepared and dispensed in a glove bag under grade 4.8 N_2, and experiments involving long-term soaking in D_2O buffer were performed in a Faraday cage placed inside the glove bag.

Results

Effect of pH. The pH meter reading (pH*) of the D_2O buffer used for voltammetric experiments was 7.2 ± 0.1, meaning that pD of these solutions is approximately 7.6 (pD ≈ pH* + 0.4).[57] On the other hand, the pH of the H_2O buffer solution was 6.9 ± 0.1 indicating that the deuterium ion concentration in D_2O buffer solution is somewhat lower than the hydronium ion concentration in the corresponding H_2O buffer solution. Avila et al. report that the electron transfer rate constant for electrostatic assemblies is pH dependent.[1] To address this concern, control experiments were performed in which the rate constant for H_2O-incubated electrostatic and covalent assemblies was initially measured in 80 mM, pH = 7 buffer, transferred to pH = 7.6 buffer of the same concentration, where k^0 was measured every twenty minutes for two hours, and then transferred back to pH = 7 buffer, where k^0 was measured every twenty minutes for two hours. In the electrostatic assemblies, the apparent rate constant increased by ~20% upon transfer to pH = 7.6 buffer; this increase was concomitant with a loss in surface coverage that ranged up to 80% after 40 min of soaking. The rate constant did not decrease significantly upon transfer back to pH = 7 buffer nor with long-term soaking in the pH = 7 buffer, indicating that the initially observed increase in the rate likely arises from the loss of weakly bound protein from the surface. For some of the covalent assemblies, the apparent rate constant increased by up to 15% following two hours in pH = 7.6 buffer, accompanied by a 15−30% loss in surface coverage; the changes were not statistically significant at 95% confidence. However, the rate constant did not decrease over time following transfer back to pH = 7 buffer, suggesting either that the initial change in pH causes a change in the adsorbed state of the protein that cannot be undone over the course of two hours in a lower pH solution; or, albeit less likely, the long-term change in the rate constant is caused by the observed loss of some residual physisorbed cytochrome *c*.

These data indicate that the pH dependence for cytochrome *c* immobilized on these mixed SAMs on smooth gold is somewhat different than in cytochrome *c* adsorbed to pure carboxylic acid SAMs on roughened silver studied by Avila et al. Similarly, Kang et al. report for cytochrome *c* electrostatically adsorbed to mixed SAMs on gold that varying the pD of the D_2O buffer used in voltammetric experiments does not affect the measured k^0.[5]

The effect of transferring cytochrome *c*/SAM assemblies from pH 8 incubant solution to pH 7 buffer was also explored by preparing assemblies in pH 8 and pH 7 incubant solution in H_2O or D_2O solvent, rinsing with buffer solution of the same pH, and then transferring the electrodes to 80 mM, pH 7 buffer of the incubant solvent. Voltammogram sets were taken every twenty minutes for two hours and k^0 was determined at each time point. The rate constant did not change in two hours of soaking for any of the H_2O-incubated assemblies. For electrostatic D_2O-incubated assemblies, the rate was seen to increase and correlate with a 40−50% decrease in surface coverage. For these assemblies, the pH dependent rise in the rate constant likely results from the loss of weakly bound cytochrome *c* from the surface.

Unless stated otherwise, the surface coverage was constant (within error) for the studies described below. In addition, the experimental method of switching a given electrode between solvent types is used to minimize differences that can occur in the sample preparation.

Cyclic Voltammetric Properties and Electron Transfer Rates. Table 1 summarizes several key properties of the cyclic voltammograms for each cytochrome *c*/SAM assembly used in this study at slower scan rates. For electrostatic and covalent assemblies, the formal potential is shifted slightly negative from that of cytochrome *c* in solution.[22] All values agree well with previously reported values.[13,16,22] Peak separations (ΔE_p) and full width at half-maximum (fwhm) values demonstrate that the protein behaves nearly ideally on the surface of the electrode; for an ideal reversible redox couple $\Delta E = 0$ mV and fwhm = 90.6 mV.[33]

Tables 2 and 3 summarize the rate constant for the different isotope combinations and the two different assemblies, electrostatic and covalent. Each scan series consists of a voltammogram set collected in cell solvent of the same isotope as the incubant followed by a voltammogram set collected in solvent of the opposite isotope; i.e., for H_2O-incubated cytochrome *c*, a scan series consisted of voltammograms to determine $k^0(H_2O, H_2O)$, followed by voltammograms to determine $k^0(H_2O, D_2O)$, while for D_2O-incubated protein, a scan series consisted of $k^0(D_2O, D_2O)$ followed by $k^0(D_2O, H_2O)$. The cytochrome *c* assemblies remained in a given cell solvent only long enough to collect a single voltammogram set, or about 90 s. In Table 2, Scan Series 1 was followed immediately by Scan Series 2

TABLE 2: Summary of Electron Transfer Rate Constants Obtained for H_2O-Incubated Cytochrome *c* Assemblies

attachment method		Scan Series 1			Scan Series 2		
		$k^0(H_2O, H_2O)$	$k^0(H_2O, D_2O)$	KIE_{cell}[c]	$k^0(H_2O, H_2O)$	$k^0(H_2O, D_2O)$	KIE_{cell}[c]
electrostatic	short chain[a]	4600 ± 400	3900 ± 400	1.2 ± 0.2	5200 ± 500	4300 ± 400	1.2 ± 0.1
	long chain[b]	600 ± 100	600 ± 100	1.0 ± 0.3	700 ± 200	800 ± 200	0.9 ± 0.2
covalent	short chain	4900 ± 1000	4000 ± 700	1.2 ± 0.3	4900 ± 900	4200 ± 500	1.2 ± 0.3
	long chain	600 ± 100	600 ± 100	1.0 ± 0.3	600 ± 100	600 ± 200	1.0 ± 0.3

[a] Corresponds to $-S(CH_2)_5COOH/-S(CH_2)_4OH$ SAMs. [b] Corresponds to $-S(CH_2)_{10}COOH/-S(CH_2)_8OH$ SAMs. [c] The ratios reported here are ratios of the average values given in the two preceding columns. Error values are obtained by propagation of the standard deviation.

TABLE 3: Summary of Electron-Transfer Rate Constants Obtained for D_2O Incubated Cytochrome *c* Assemblies

attachment method		Scan Series 1			Scan Series 2		
		$k^0(D_2O, D_2O)$	$k^0(D_2O, H_2O)$	KIE_{cell}	$k^0(D_2O, D_2O)$	$k^0(D_2O, H_2O)$	KIE_{cell}
electrostatic	short chain	2900 ± 400	3700 ± 700	1.3 ± 0.3	3200 ± 400	3700 ± 500	1.2 ± 0.2
	long chain	500 ± 100	500 ± 200	1.1 ± 0.5	400 ± 100	500 ± 100	1.1 ± 0.3
covalent	short chain	3500 ± 400	4200 ± 400	1.2 ± 0.2	3600 ± 500	4300 ± 400	1.2 ± 0.2
	long chain	700 ± 100	700 ± 100	1.0 ± 0.2	700 ± 70	700 ± 90	1.1 ± 0.2

with the same electrode. At 95% confidence, Scan Series 1 and Scan Series 2 are the same in a given solvent, indicating that the resulting isotope effect, termed KIE_{cell}, is fully reversible on short time scales.

For $-S(CH_2)_{10}COOH/-S(CH_2)_8OH$ cytochrome *c*/SAM assemblies, which corresponds to the tunneling region, the rate constant does not vary with the isotope of the cell or incubant solution. Statistical analysis (*t*-test) confirms this observation: at 99% confidence, the average rate in H_2O did not significantly differ from the rate in D_2O. This result is consistent with an electron transfer rate that is determined by the tunneling probability, i.e., the thickness of the SAM layer and is corroborated by previous studies of Py-terminated[6] and electrostatically adsorbed cytochrome *c* on pure $-COOH$-terminated monolayers.[7]

In contrast to the long-chain cytochrome *c*/SAM assemblies, the electron transfer rate in $-S(CH_2)_5COOH/-S(CH_2)_4OH$ cytochrome *c*/SAM assemblies, corresponding to the plateau region, depends on the isotope of the cell and incubant solutions. Figure 2 shows typical voltammograms obtained for H_2O-incubated short-chain SAM/cytochrome *c* assemblies using the electrostatic adsorption and covalent attachment methods. Both slow scan rates (row i) and fast scan rates (row ii) are shown, in H_2O buffer (red) and in D_2O buffer (blue). The curve in row iii of each panel shows the fit assigned to the data collected in H_2O (closed symbols) according to the Marcus density of states treatment; open symbols are for the D_2O cell solution. The fit was determined as an average of the fits to the anodic and cathodic waves, which differed by no more than ± 15%. The α values for each assembly are close to 0.5, indicating that the voltammetric waves are symmetric and that the electrochemical reaction is quasi-reversible.

At the slowest scan rate of 10 V/s (row i of Figure 2), it is evident that, aside from a slight drop in peak current, which would seem to indicate the desorption of some protein from the electrode surface, the voltammetry of the protein is similar, if not identical, in H_2O or D_2O cell solvent. The small peak separation indicates that the electron transfer process remains quasi-reversible after the quick transfer from H_2O to D_2O buffer. The position of the peaks does not change when the switch is made from H_2O to D_2O solution, indicating that $E^{0\prime}$ remains the same and thus there is no appreciable change to the stability or strength of the bound state of the protein as a function of the cell solvent. A study by Battistuzzi et al.[2] has addressed these thermodynamic questions in detail and reports that, although H/D substitution produces substantial changes in the redox enthalpy and entropy, these effects largely compensate and lead to no net effect on $E^{0\prime}$.

At the higher scan rate of 1000 V/s (row ii of Figure 2) it becomes evident that the electron transfer rate constant is slower in D_2O buffer than in H_2O for electrostatic and covalent assemblies. This difference is evident from the larger separation and width of the peaks in D_2O. This slowing is even more apparent upon examination of row iii, which shows the plot of peak separation versus the scan rate. The voltammetric peaks for electrostatic and covalent systems in D_2O cell solvent (open symbols) diverge more quickly than those collected in H_2O cell solvent (closed symbols), which results in fitting the data with a smaller rate constant. On average, $k^0(H_2O, D_2O)$ is approximately 20% smaller than that in $k^0(H_2O, H_2O)$ for short chain assemblies. This effect is called KIE_{cell} and is summarized in Tables 2 and 3.

Statistical analysis indicates that KIE_{cell} is significant in short chain systems; at 95% confidence, the rate in the solvent is significantly different from the rate in the countersolvent for H_2O- and D_2O-incubated electrostatic and covalent assemblies. It is also reversible, as there is no significant difference in the rate constant between scan sets in a given solvent. It is of interest to note that these ratios are similar to those obtained by Murgida and Hildebrandt using SERRS to monitor the electron transfer rate of H_2O- and D_2O-incubated cytochrome *c* electrostatically adsorbed to pure $-COOH$ terminated SAMs on Ag electrodes.[7]

The incubant effect, referred to here as KIE_{inc}, was evaluated by comparing $k^0(H_2O, H_2O)$ to $k^0(D_2O, H_2O)$. This comparison was made to remove the contribution of the increased viscosity of D_2O, *vide infra*. From Table 4, it is clear that an incubant effect occurs in both the electrostatic and covalent systems, and that it is comparable to KIE_{cell} in magnitude. These data indicate that, at longer time scales, H/D exchange in the protein matrix also contributes to slowing of the electron transfer rate, as reflected by a smaller measured rate constant in D_2O incubant.

An isotope effect, KIE_{total}, that results from the combined effects of cell and incubant isotopes is also readily observed by comparing $k^0(H_2O, H_2O)$ to $k^0(D_2O, D_2O)$. This effect is larger than either KIE_{cell} or KIE_{inc} and is equal to the product of the two effects (given as $KIE_{total, pred}$ in Table 4).

Viscosity Effect on Rate. It has been observed that the electron transfer rate constant is affected by solution viscosity in the plateau region.[1,6,16] Because no study reports the dependence of the rate constant on viscosity for covalent systems

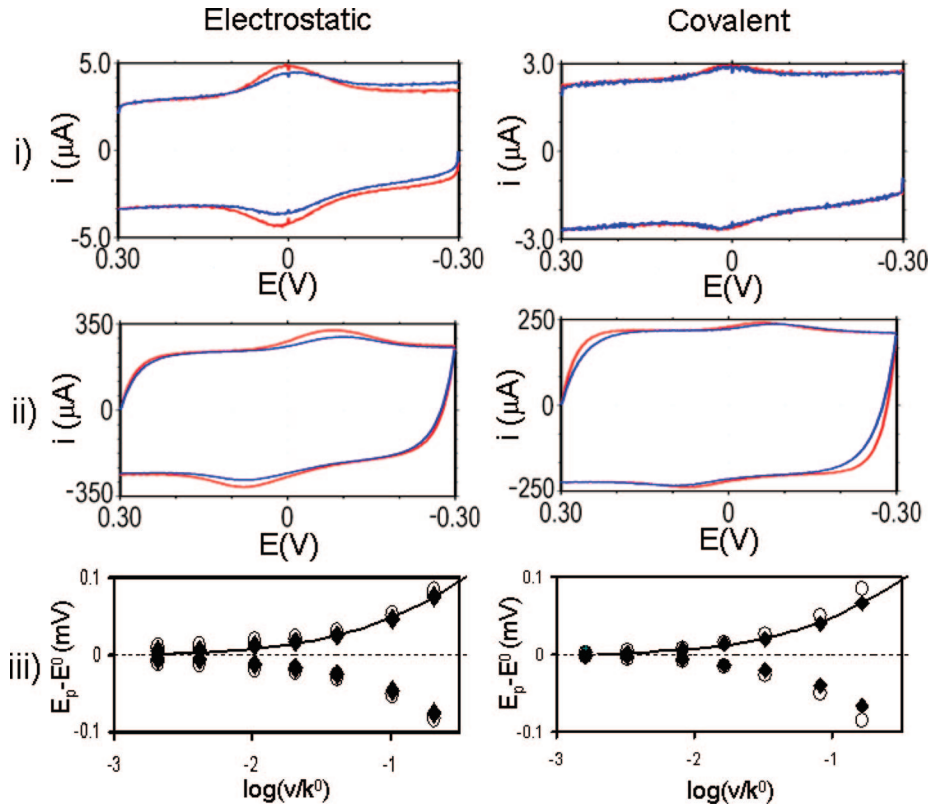

Figure 2. Representative cyclic voltammograms and kinetic information for short-chain electrostatic (left) and covalent (right) H_2O-incubated cytochrome *c*/SAM assemblies on Au electrodes. Each column reports data collected on a single electrode of each assembly type. Red lines correspond to voltammograms collected in H_2O buffer; blue lines correspond to voltammograms collected in D_2O buffer. (i) Voltammograms collected at 10 V/s. (ii) Voltammograms collected at 1000 V/s. (iii) Plots of peak potential vs scan rate from $\upsilon = 10$ to 1000 V/s. Closed diamonds correspond to voltammograms collected in H_2O, while open circles correspond to voltammograms collected in D_2O. The solid curve is the Marcus theory fit to the data with $\lambda = 0.6$ eV and $k^0(H_2O, H_2O) = 5000\ s^{-1}$ for the electrostatic system and $\lambda = 0.6$ eV and $k^0(H_2O, H_2O) = 6000\ s^{-1}$ for the covalent system. A dashed line at $y = 0$ is included for convenience. The voltammetry for D_2O-incubated cytochrome *c* assemblies was equally regular.

TABLE 4: Evaluation of the Kinetic Isotope Effects Observed for Short Chain Cytochrome *c*/SAM Assemblies

	electrostatic[a]	covalent[a]
KIE_{cell}[b]	1.2 ± 0.2	1.2 ± 0.2
KIE_{inc}[c]	1.3 ± 0.3	1.1 ± 0.2
$KIE_{total,}$[c]	1.6 ± 0.3	1.4 ± 0.3
$KIE_{total,\ pred}$[d]	1.6 ± 0.4	1.4 ± 0.4

[a] All values reported from the average of the scan sets in a given solvent. [b] obtained by comparing the average values of $k^0(H_2O, H_2O)$ to $k^0(H_2O, D_2O)$. [c] obtained by comparing the average values of $k^0(H_2O, H_2O)$ to $k^0(D_2O, H_2O)$. [c] obtained by comparing the average values of $k^0(H_2O, H_2O)$ to $k^0(D_2O, D_2O)$. [d] $KIE_{total,\ pred.} = KIE_{cell} \times KIE_{inc}$. Error obtained by propagating the standard error in KIE_{cell} and KIE_{inc}.

or mixed $-S(CH_2)_mCOOH/-S(CH_2)_nOH$ systems, it was measured for $k^0(H_2O, H_2O)$ in H_2O buffer solutions modified using dextrose (1.0−2.5 cP at room temperature). The k^0 data were fit to the empirical form $\eta^{-\lambda}$ where $0 \leq \lambda \leq 1$.[14] The best fit line was established using weighted linear regression.[34] For the electrostatic case, this analysis yielded $\lambda = 1.1$, while in the covalent systems the value was $\lambda = 1.0$.

Figure 3 shows plots of the electron transfer rate constant as a function of viscosity for electrostatic and covalent systems. The closed points show the measured viscosity dependence of electrostatic (panel A, squares) and covalent (panel B, triangles) assemblies. The acceptable best-fit region of the viscosity dependence, as determined by contour plots of χ^2 goodness-of-fit values (see Supporting Information) are shown by the hashed regions. The open diamonds correspond to $k^0(H_2O, D_2O)$, and the open circles to $k^0(D_2O, D_2O)$ respectively, for each assembly type. From this plot, it is apparent that the upper limits of $k^0(H_2O, D_2O)$ for both assemblies are located in or near the best-fit viscosity region, while $k^0(D_2O, D_2O)$ is not located in the viscosity dependent region, indicating that H/D exchange affects the rate constant at longer exposure time.

To further demonstrate that the observed isotope effect is caused by the viscosity difference between the two solvents, 80 mM phosphate buffer was adjusted to a viscosity of 1.09 cP with 70 g/L glucose, which is comparable to the viscosity of pure D_2O (1.0961 cP at 25 °C). Using cytochrome *c* electrostatically absorbed to $-S(CH_2)_5COOH$ /$-S(CH_2)_4OH$ SAMs, solvent switching experiments were then performed between unadjusted H_2O buffer and viscosity-adjusted H_2O buffer. The results of these experiments are shown in Table 5. Comparison of $k^0(H_2O, H_2O)$ to $k^0(H_2O$, viscous $H_2O)$ yields ratios that are similar to those found for $k^0(H_2O, H_2O)$ to $k^0(H_2O, D_2O)$, supporting the interpretation that the observed change in the rate constant caused by the cell solution is controlled by viscosity rather than H/D exchange.

Time Scale of the Incubant Effect at Short-Chain SAMs. The dependence of the rate constant on H/D exchange in cytochrome *c*/short-chain SAM assemblies was examined by performing soaking experiments in which an electrode was allowed to remain in the countersolvent for an extended period of time. Figure 4 shows the results of these experiments. An initial rate constant was measured in the incubant solvent (closed symbols, H_2O-incubated; open symbols, D_2O-incubated), after which the electrode was transferred to the countersolvent and

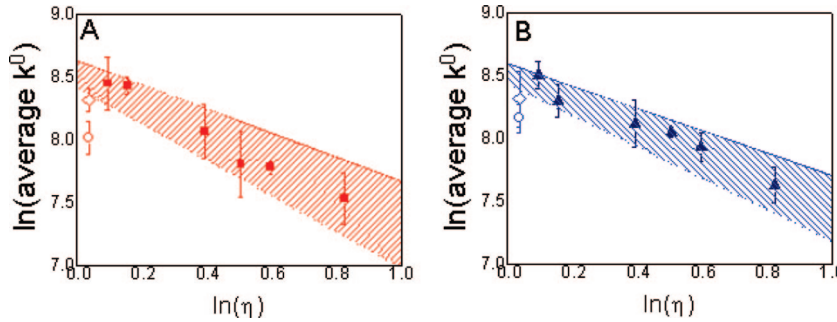

Figure 3. This figure plots the electron transfer rate constant versus the logarithm of solution viscosity for electrostatic (panel A) and covalent (panel B) assemblies. Open diamonds correspond to $k^0(H_2O, D_2O)$, while open circles correspond to $k^0(D_2O, D_2O)$. The hashed regions show the best-fit region as a result of χ^2 goodness-of-fit analysis of the weighted linear regression of $k^0(H_2O$, viscous water), which is plotted as closed squares for electrostatic systems and closed triangles for covalent systems.

TABLE 5: Summary of Cell and Incubant Effects and Comparison to Viscosity Effect[a]

	incubant solvent, cell solvent	k^0(incubant, cell): $k^0(H_2O, H_2O)$
electrostatic	H_2O, D_2O[a]	1.2 ± 0.2
	H_2O, viscous H_2O	1.1 ± 0.3
covalent	H_2O, D_2O[a]	1.2 ± 0.3
	H_2O, viscous H_2O	1.2 ± 0.2

[a] Evaluated from the k^0 value measured in the first scan series of each switching experiment. [a] Referred to as KIE_{cell} in the text.

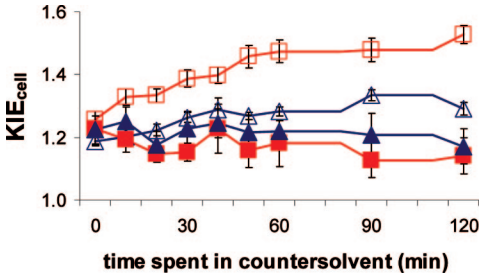

Figure 4. Effect of countersolvent soaking on the electron-transfer rate for electrostatic (red) and covalent (blue) assemblies. Filled symbols represent H_2O-incubated assemblies and open symbols represent D_2O-incubated assemblies. The ratio KIE_{cell} is the ratio of the initial rate constant measured in the incubant solvent to the rate constant measured in the countersolvent.

successive rate constant measurements were made at ten minute intervals for the first hour, and thirty minute intervals for the second hour. The ratio between the rate constant measured at a given time point and the initial measurement in the incubant solvent, KIE_{cell}, is plotted on the *y*-axis. From Figure 4, it is evident that for covalent assemblies, either H_2O-incubated or D_2O-incubated, KIE_{cell} does not change on the time scale of these experiments. The results of *t*-tests at 99% confidence confirm that no significant difference is present between KIE_{cell}(0 min) and KIE_{cell} at any other time point. The H_2O-incubated covalent assemblies and D_2O-incubated covalent assemblies do not show any change in surface coverage with soaking time.

The rate constant for the electrostatic assemblies changes with the solvent, however. For D_2O-incubated assemblies that are transferred into a H_2O cell solution, KIE_{cell} increases from an initial value of 1.3 to a final value of 1.5 at 2 h, which is equal to the KIE_{cell} and KIE_{total} values reported in Table 4, within error. A *t*-test at 99% confidence shows that KIE_{cell} at any time point >50 min is significantly different from KIE_{cell}(0 min). No significant (*t* test with 99% confidence) change in the surface coverage for the D_2O-incubated electrostatic assemblies is observed. For H_2O-incubated assemblies that are transferred into a D_2O cell solution, the isotope effect does not change significantly and remains 1.2. The loss of surface bound cytochrome *c* was, however, statistically significant for H_2O-incubated electrostatic assemblies soaked in D_2O and is in agreement with the pH to pD shift (see above). The onset of KIE_{inc} may be at least partially masked by a shift in the apparent rate constant arising from the desorption of weakly bound cytochrome *c*; however, the extent of this effect is not certain, especially given that it is not observed for H_2O-incubated covalent assemblies or D_2O-incubated assemblies in general These data indicate that the rate of D/H exchange in electrostatic assemblies is faster than the H/D exchange rate, and that the onset of the KIE for D/H exchange occurs at approximately 50 min upon reverse exchange for this particular assembly.

Using SERRS, Hildebrandt et al. have previously observed that the H/D exchange processes related to structural changes in the heme pocket of yeast cytochrome *c*, which would presumably affect the electron transfer rate, are complete within 24 h, though the most pronounced structural changes are complete in <15 min.[4] From our experiments, however, we can assign a lower time limit of about 2 h to any H/D exchange process that affects the rate in covalent assemblies. Considering the close similarity in the composition,[24,39] electrochemical properties, and electron transfer rate constants[17,21,22] of the two assemblies, this time limit seems probable for electrostatic assemblies as well. This conclusion is similar to that reached by Kang et al., who report that, for cytochrome *c* electrostatically adsorbed on mixed $C_{10}COOH/C_6OH$ SAMs, the apparent rate constant begins to decrease after 24 h and continues to decrease for up to 72 h soaking in D_2O.

We find that any "important" protons participating in electron transfer are likely to exchange with deuterium on a time scale of 2−24 h.

Discussion

Effect of pH. The impact of the hydronium and deuterium ion concentrations on the electron transfer rate constant was assessed. The pH effect was explored in an analogous system in which H_2O-incubated cytochrome *c*/SAM assemblies were soaked in higher pH buffer, for which the pH of the H_2O buffer solution was equal to the pD of the D_2O buffer used in voltammetric experiments. In both electrostatic and covalent assemblies, the apparent rate constant increased upon transfer to pH = 7.6 buffer; this increase was concomitant with a loss in surface coverage, up to 80% for electrostatic assemblies and up to 30% for covalent assemblies. In neither case did the rate constant change upon return to pH = 7 buffer for an additional two hours of soaking, indicating that the initially observed

increase in the rate likely arises from the loss of weakly bound protein from the surface. These results suggest either that the initial change in pH causes a change in the adsorbed state of the protein that cannot be undone over the course of two hours in a lower pH solution, or that the change in the rate constant is caused by the observed loss of some residual physisorbed cytochrome *c*.

These data indicate that the pH dependence for cytochrome *c* immobilized on these mixed SAMs on smooth gold is somewhat different than in cytochrome *c* adsorbed to pure carboxylic acid SAMs on roughened silver studied by Avila et al. Indeed, it has been demonstrated that the surface topography of the SAM, which is influenced by both SAM composition and substrate roughness, can greatly affect the adsorbed state of cytochrome *c*,[41,45] and so it is reasonable to postulate that cytochrome *c* may behave differently in the systems studied here as opposed to those studied by Avila et al. Kang et al. have reported that varying pD (pD $\approx$ pH* + 0.4) of the D_2O buffer does not affect the measured k^0, also indicating that the pH dependence of cytochrome *c* for mixed SAMs on gold may differ from cytochrome *c* adsorbed to mixed SAMs on silver. Furthermore, in this study the rate constant was seen to increase for cytochrome *c* upon transfer to higher pH buffer, whereas the rate constant was seen to decrease upon transfer to D_2O, indicating that some other effect (viscosity at short time scales, H/D exchange at $t > 2$ h) is responsible for the observed decrease in the rate constant in D_2O solution.

KIE_{cell} Is a Viscosity Effect. Previous work[6,16,17,21] suggests that, for cytochrome *c* immobilized to thin SAMs, electron transfer is coupled to the polarization response of the medium, which includes the protein interior and its environment. If such a mechanism is operative for electrostatic and covalent assemblies, then adjustment of solvent friction via solution viscosity should affect the electron transfer rate, an observation that has already been made for cytochrome *c* electrostatically adsorbed to thin, pure $-$COOH-terminated SAMs[1] and coordinatively bound via the heme iron to thin, pyridine-terminated SAMs.[6]

Zusman[35,36] has developed a unified expression for electron transfer that includes the effects of solvent friction for the rate constant of a reduction process at a metal electrode:

$$k_{red} = k_{NA}\left[1 + \pi\tau_s k_{NA}\sqrt{\frac{\pi k_B T}{\lambda}}\frac{\exp(\Delta G^{\ddagger}/k_B T)}{\sin(\pi\sqrt{2\lambda/\Delta G^{\ddagger}})}\right]^{-1} \quad (1)$$

In this expression, τ_s is the characteristic polarization relaxation time of the medium and λ is the reorganization energy. The activation energy $\Delta G^{\ddagger}$ is defined as $\Delta G^{\ddagger} = (e(E - E^0) + \lambda)^2/4\lambda$, where E is the electrode potential, and E^0 is the standard potential of the redox couple. k_{NA} is the rate constant in the nonadiabatic limit and is expressed as

$$k_{NA} = \frac{\pi}{\hbar}\frac{|V|^2\rho}{\sqrt{\pi k_B T}}\int_{-\infty}^{\infty}\exp\left[-\frac{(\lambda + (\varepsilon_F - \varepsilon) + e(E - E^0))^2}{4\lambda k_B T}\right]\times \frac{1}{1 + \exp[(\varepsilon - \varepsilon_F)/k_B T]}\,d\varepsilon \quad (2)$$

where $|V|$ is the magnitude of the electronic coupling between states in the electrode and the protein's redox center, ρ is the density of electronic states in the electrode, and ε_F is the energy of the Fermi level.

We simplify eq 1 by considering the plateau region to correspond to the friction control limit. In the friction-controlled limit, $k_{NA} \gg (1/\pi\tau_s)\sqrt{(\lambda/\pi k_B T)}\,\sin(\pi\sqrt{(\Delta G^{\ddagger}/2\lambda)})\,\exp(-\Delta G^{\ddagger}/k_B T)$ so that eq 1 simplifies to

$$k_{fc} = \frac{1}{\pi\tau_s}\sqrt{\frac{\lambda}{\pi k_B T}}\sin\left(\pi\sqrt{\frac{\Delta G^{\ddagger}}{\lambda}}\right)\exp\left(-\frac{\Delta G^{\ddagger}}{k_B T}\right) \quad (3)$$

From eq 3, the electron transfer rate constant is inversely proportional to the characteristic polarization relaxation time τ_s. The solution viscosity η can be related to τ_s through the longitudinal relaxation time τ_L as given by Debye's model:[36]

$$\tau_s \approx \tau_L = \left(\frac{\varepsilon_\infty}{\varepsilon_s}\right)\frac{3\eta V_m}{RT} \quad (4)$$

where ε_∞ and ε_s are the high-frequency and static dielectric constants of the solvent, respectively, and V_m is the molar volume. In this model, the viscosity dependence has the form $k^0 \propto \eta^{-1}$; this form agrees with the viscosity dependence observed for the electrostatic and covalent systems here and with that reported earlier by Avila et al. for cytochrome *c* electrostatically adsorbed to thin carboxylic acid-terminated SAMs.[1] The static and high-frequency dielectric constants of H_2O and D_2O differ by less than 1%, and so the effect of the dielectric constant term in eq 4 is negligible.

Since eq 3 predicts an inverse relationship between k^0 and τ_s, and the assemblies used in this study show this dependence (see Figure 3 and Supporting Information), an expression of KIE_{cell} that only takes into account the viscosity of H_2O and D_2O cell solutions can be constructed as follows

$$\frac{k^0(H_2O, H_2O)}{k^0(H_2O, D_2O)} \propto \frac{\tau_s(D_2O)}{\tau_s(H_2O)} \propto \frac{\eta(D_2O)}{\eta(H_2O)} \quad (5)$$

Using the measured viscosities of 0.929 cP for the 80 mM H_2O phosphate buffer and 1.030 cP for the 80 mM D_2O phosphate buffer, the theoretical value of $k^0(H_2O)$:$k^0(D_2O)$ is 1.11, and agrees well with the KIE_{cell} values for electrostatic and covalent assemblies given in Table 5. Furthermore, $k^0(H_2O, H_2O)$:$k^0(H_2O$, viscous $H_2O)$ is also given in Table 5 and agrees well with KIE_{cell}. Figure 3, which plots $k^0(H_2O, D_2O)$ with the results of $k^0(H_2O$, viscous $H_2O)$ shows that, within error, $k^0(H_2O, D_2O)$ is located within the viscosity-dependent regime, albeit slightly lower. These results indicate that KIE_{cell} most likely arises from the viscosity difference between the solvents and cannot rightly be called an isotope effect.

Incubant Isotope Effect and Total Isotope Effect. From Table 4 and Figure 3, it is clear that, on long time scales (>2 h) the decrease in the rate constant arising from the higher viscosity of D_2O is augmented by some other process, presumably H/D exchange of some protein residues or of one or more catalytic water molecule(s) present in the heme cleft.[4,37,38] The contribution of this effect can be separated from KIE_{total} by comparing $k^0(H_2O, H_2O)$ to $k^0(D_2O, H_2O)$, thus removing the effect of the more viscous D_2O cell solution from the analysis. The resulting effect, termed KIE_{inc}, is similar in magnitude to KIE_{cell}; however, KIE_{inc} in electrostatic assemblies is larger ($KIE_{inc} = 1.3$) than in covalent assemblies ($KIE_{inc} = 1.1$). This difference may indicate that specific bonded contacts between cytochrome *c* and the SAM are less important to the electron transfer process for covalent complexes than for electrostatic complexes. However given that the KIE_{inc} for the electrostatic assemblies and the KIE_{inc} for covalent assemblies are comparable (within error) and the close similarity in the composition,[24,39] electrochemical properties, and electron transfer rate constants[17,21,22] of the two assemblies, any difference appears to be slight.

The cell and incubant effects combine in a multiplicative fashion to form the total kinetic isotope effect; that is, KIE_{cell}

$\times$ $KIE_{inc} = KIE_{tot}$. This observation can be rationalized in terms of eq 3 by taking the activation energy $\Delta G^{\ddagger}$ to be $\lambda/4$ and approximating the reorganization energy, λ, as classical. These approximations yield the following expression for the standard rate constant k^0:

$$k_{fc}^0 \approx \frac{1}{\pi\tau_s}\sqrt{\frac{\lambda}{\pi k_B T}}\exp\left(-\frac{\lambda}{4k_B T}\right) \quad (6)$$

The solution viscosity is expected to affect mainly the characteristic polarization relaxation time τ_s and not the other terms, which are energetic rather than dynamical. This factor accounts for the cell solvent dependence in the preexponential term of eq 6. In the context of eq 6, the presence of a separate KIE_{inc} implies that H/D exchange increases the reorganization energy somewhat, a finding that seems plausible, *vide infra*. We assume that H/D exchange effects are contained within the reorganization energy λ, which primarily affects the exponential term in eq 6. By these criteria, in order to produce a KIE_{inc} of 1.2, which would in turn result in a KIE_{tot} of 1.4, the difference between λ_{H_2O} and λ_{D_2O} would need to be 4 meV. While plausible, such a small difference in reorganization energy would be difficult to demonstrate experimentally.

Previous isotope effect studies. Several studies have already been conducted and hypotheses developed to explain the isotope dependence of the electron transfer rate constant at short distances. Using cytochrome *c* electrostatically adsorbed to pure $-$COOH-terminated SAMs of varying length, Murgida and Hildebrandt[7] observed a total kinetic isotope effect $k^0(H_2O, H_2O):k^0(D_2O, D_2O)$ at short distance ($m < 5$). The magnitude of the effect increased from 1.2 at a $-S(CH_2)_5COOH$ SAM to 4.0 at a $-S(CH_2)COOH$ SAM. From these observations, they hypothesized that electron transfer is coupled with proton transfer, and that the proton transfer step becomes rate-limiting for thin SAMs. The strength of the applied electric field, which is larger for thin SAMs, may also increase the activation energy for proton transfer,[7] raising the protein's contribution to the reorganization energy in the rearrangement of the hydrogen bonding network involved with electron transfer. Since the energy required to rearrange a hydrogen bonding network is larger for D_2O than H_2O, a kinetic isotope effect would be observed.

The isotope effects observed in this study for electrostatic and covalent assemblies on mixed $-S(CH_2)_5COOH/-S(CH_2)_4OH$ SAMs agree well with those reported by Murgida and Hildebrandt for electrostatic cytochrome *c* at pure $-S(CH_2)_5COOH$ SAMs; see Table 4. It is interesting to note, however, that they appear to observe KIE_{cell} on their experimental time scale (45 min); according to Table 4, a KIE of $\sim$1.6 should be expected at a $-S(CH_2)_5COOH$ SAM if KIE_{inc} were also present. For increasingly thinner SAMs, however, the KIE continues to increase, though the experimental time is held constant. This observation may indicate that the onset of KIE_{inc} is faster for thinner SAMs and begins to contribute to the observed KIE sooner.

Khoshtariya et al.[6] report that, for cytochrome *c* ligated to the pyridine terminus of a $-S(CH_2)_{11}Py/-S(CH_2)_9CH_3$ SAM (representative of the plateau region), the rate deceases by $\sim$30% when the protein is exposed to D_2O for 30 min or more, while brief exposure results in no change in the rate. No isotope effect was observed for cytochrome *c* on $-S(CH_2)_{16}Py/-S(CH_2)_{14}CH_3$ SAMs (tunneling regime). These results suggest a change in the electron transfer mechanism with distance. The hypothesis was made that at short distances a friction-controlled mechanism for electron transfer is operative in which electron transfer is coupled to the polarization response of the medium, including the protein interior and its environment. This hypothesis is consistent with our findings: we also observe a change in the isotope effect with SAM thickness, and we further observe a D_2O viscosity-induced effect that is consistent with a friction-control mechanism such as that in eq 3. The same D_2O viscosity dependence was not observed in Khoshtariya's study; however, the viscosity dependence was found to be weaker for the pyridine-ligated systems, taking the form $k^0 \propto \eta^{-\lambda}$ where $\lambda = 0.58$ for $-S(CH_2)_{11}Py/-S(CH_2)_9CH_3$ films and $\lambda = 0$ for $-S(CH_2)_{16}Py/-S(CH_2)_{14}CH_3$ films.[6]

Most recently, Kang et al.[5] studied solvent isotope effects in single crystal zinc cytochrome *c* porphyrin:yeast cytochrome *c* complexes by transient absorption spectroscopy and for yeast cytochrome *c* electrostatically adsorbed to $-S(CH_2)_{10}COOH/-S(CH_2)_6OH$ SAMs on gold electrodes. They observed that upon soaking, H_2O-prepared films and crystals underwent two distinct processes: an initial acceleration of the electron transfer rate upon exposure to the solvent, followed by a prolonged decrease in the rate constant at times up to 72 h. The first process was attributed to changes in the compressibility of the protein between the two solvents, while the second process was ascribed to slowly exchanging, protected solvent molecules within the protein, thereby altering the protein/SAM interactions. Furthermore, it was hypothesized that H_2O and D_2O may cause adsorption states of cytochrome *c* that are subtly different from one another (only a slight difference in voltammetric properties was observed between H_2O- and D_2O-prepared films), causing the electron transfer rate to be slower, and the long-term decline in the rate constant was associated with a conversion between those states, rather than to the exchange of specific protons.

It should be noted that no other author reports an initial acceleration nor a long-term decrease in the rate constant for a SAM containing $-S(CH_2)_{10}COOH$ or any other component representative of the tunneling regime, as was observed by Kang et al.. An initial increase in rate upon transfer to D_2O could result from a loss of weakly bound cytochrome *c* from the electrode surface, leaving more strongly bound species with a faster rate. In our experiments with electrostatically adsorbed protein, we found it necessary to use a bias potential of $+0.3$ V between experiments to prevent such a loss. Neither was the analogous behavior observed for short-chain SAMs; immediately upon exposure to D_2O buffer, the rate constant either immediately decreased or remained the same.[6]

The observation of a long-term isotope effect in Kang's study may arise from the large length difference (four methylene groups) between the $(CH_2)_{10}COOH$ component which binds the cytochrome *c* and the $(CH_2)_6OH$ diluent. Mixed SAMs with components of different lengths have been shown to present a "rougher" binding surface for cytochrome *c*[40,41] and also provide alternative tunneling pathways.[21,42,43] It is also conceivable that small solvent molecules can be trapped in such films, so that over time, the character of the SAM-protein interface changes with exposure to D_2O, leading to the observed slowing of the rate. Furthermore, binding in the electron transfer complex formed by yeast cytochrome *c* with cytochrome *c* porphyrin has been shown to be primarily hydrophobic in nature.[44] This feature seems to be preserved at $-$COOH-terminated SAMs; changing the SAM composition to include an $-$OH-terminated diluent results in drastic rate enhancement, even more so than in the case of horse heart cytochrome *c*.[45] Therefore, the adsorbed state of yeast cytochrome *c* in the mixed $-S(CH_2)_{10}COOH/-S(CH_2)_6OH$ films used by Kang et al. may be different

than in other studies involving horse heart cytochrome *c* and may contribute to their observed isotope effect.

Is Electron Transfer Coupled with Proton Transfer? Electron transfer and proton-coupled electron transfer (PCET) mechanisms exist in direct competition for electron donor−acceptor systems separated by a hydrogen-bonded network.[46−50] Hammes-Schiffer and co-workers have developed a theoretical description for such systems, in which the rate constant expression has the form

$$k = \frac{2\pi}{\hbar}\sum_{\mu} P_{I\mu}\sum_{\nu} V_{\mu\nu}{}^{2}(4\pi\lambda_{\mu\nu}k_{B}T)^{-1/2}\exp\left\{\frac{-(\Delta G^{\circ}_{\mu\nu}+\lambda_{\mu\nu})}{4\lambda_{\mu\nu}k_{\mathrm{B}}T}\right\} \quad (7)$$

$|V_{\mu\nu}|$ is the coupling between the reactant and product states and is defined as the average of the quantity $V(r_{\mathrm{p}}, z_{\mathrm{p}})$, which is a linear combination of couplings between four diabatic states that are weighted depending on the proton coordinate r_{p}, and z_{p} is the solvent-proton interaction coordinate. As a result, $|V_{\mu\nu}| \ll kT$ for most PCET reactions, even if electron transfer is adiabatic.[48] The solvent reorganization energy $\lambda_{\mu\nu}$ and the reaction free energy $\Delta G^{\circ}_{\mu\nu}$ are generalizations of the Marcus theory parameters for electron transfer to a combined proton and electron transfer process. $P_{I\mu}$ is the Boltzmann factor for the reactant state. Decornez and Hammes-Schiffer[51] examined several model systems and showed how the dominant mechanism (electron transfer alone (ET), concerted electron and proton transfer (EPT), or electron transfer followed by proton transfer) changes with the electron donor−acceptor distance, proton donor−acceptor distance, and the reaction free energy. The results suggest that for pure ET the KIE is nearly unity, but it increases in magnitude as the contribution of the EPT channel increases. This factor increases with reaction endothermicity, decreasing solvent polarity and decreasing donor−acceptor distance.

This model provides a way to understand our observations for KIE_{inc} and KIE_{tot} as well as those of Murgida and Hildebrandt. At long distances, the rate-limiting step is pure electron transfer and the KIE is unity, as demonstrated by measurements of the KIE for cytochrome *c*/SAM systems having >7 methylenes. As the thickness of the tunneling barrier decreases, the KIE increases steadily from 1.2 at $n = 5$ methylenes to 4.0 at $n = 1$ methylenes, indicating that an increasing dependence on a PCET mechanism may occur as the cytochrome *c*/electrode distance decreases.

Possible Residues Involved in Electron Transfer. As noted above, any exchangeable protons that participate in a PCET process exchange on the time scale of 2−24 h. In a summary of their work on hydrogen exchange in horse heart cytochrome *c*, Englander and co-workers[52] list the exchange rates for fifty-four backbone NH residues and two side chain NH groups. Twenty-four backbone NH and one side chain NH exchange on this time scale, including some residues that are important to redox-linked structural changes[4,37,38,53−55] such as Met18, Thr19, Trp59 and Tyr67, which are known to interact with internal water molecules and/or the heme group. Specific protons that are "important" to the electron transfer cannot be confidently identified for two reasons. The first is that the small magnitude of the isotope effect itself strongly suggests that there are no important protons to be identified. The second is that, even for the residues listed above, most of the relevant hydrogen-bonded interactions take place via side chain interactions rather than backbone interactions. This includes the cytochrome *c*/SAM interface, which is formed via interactions between the carboxylate-termini of the SAM and side chain NH_2 groups on lysine residues.[20,24] The exchange rates for such side chain residues are largely unavailable save the two reported by Englander. Because hydrogens known to participate in structural hydrogen bonds are known to exchange more slowly than residues that do not participate in secondary structural interactions,[56] it would be necessary to measure the exchange rates of such side chain protons for cytochrome *c* in an electron transfer complex rather than free protein. If there were specific individual protons responsible for setting the conformation of the electron transfer complex or involved in a dominant electron transfer pathway, they would likely be involved in structural hydrogen bonding, rendering measurements of the exchange rate of the free proton meaningless.

Conclusions

For electrostatic and covalent cytochrome *c*/SAM assemblies in which the SAM is thin, two separate H/D isotope effects are evident: a cell isotope effect, which results when the solvent is replaced with D_2O, and an incubant isotope effect, which results from allowing hydrogens in the protein to exchange with deuterium. Both effects are comparable in magnitude and are small (∼1.2). The cell effect can be attributed to the increased viscosity of D_2O relative to H_2O and cannot rightly be called an isotope effect. The incubant effect appears on a time scale of 2−24 h and seems too small to result from the exchange of a specific proton or protons; however, further measurements of the exchange rates of side chain protons involved in hydrogen-bonding interactions relevant to the electron transfer process are needed to elucidate whether those protons exchange on the relevant time scale. The contribution of a proton-coupled electron transfer channel may exist, and its importance may increase as the protein-SAM distance decreases.

Acknowledgment. We thank the US National Science Foundation (CHE-0415457 and CHE-0718755) for providing support for this work. We are also grateful to Jessica Davis for some initial experimental work.

Supporting Information Available: Text and figure showing the χ^2 goodness-of-fit method for determining viscosity-dependent region for electrostatic and covalent assemblies. This material is available free of charge via the Internet at http://pubs.acs.org.

References and Notes

(1) Avila, A.; Gregory, B. W.; Niki, K.; Cotton, T. M. *J. Phys. Chem. B* **2000**, *104*, 2759–2766.
(2) Battistuzzi, G.; Borsari, M.; Ranieri, A.; Sola, M. *J. Biol. Inorg. Chem.* **2004**, *9*, 781–787.
(3) Feng, Z. Q.; Imabayashi, S.; Kakuichi, T.; Niki, K. *J. Chem. Soc., Faraday, Trans.* **1997**, *93*, 1367–1370.
(4) Hildebrandt, P.; Vanheck, F.; Heibel, G.; Mauk, A. G. *Biochemistry* **1993**, *32*, 14158–14164.
(5) Kang, S. A.; Hoke, K. R.; Crane, B. R. *J. Am. Chem. Soc.* **2006**, *128*, 2346–2355.
(6) Khoshtariya, D. E.; Wei, J.; Liu, H.; Yue, H.; Waldeck, D. H. *J. Am. Chem. Soc.* **2003**, *125*, 7704–7714.
(7) Murgida, D. H.; Hildebrandt, P. *J. Am. Chem. Soc.* **2001**, *123*, 4062–4068.
(8) Murgida, D. H.; Hildebrandt, P. *J. Mol. Struct.* **2001**, *565−566*, 97–100.
(9) Murgida, D. H.; Hildebrandt, P. *Acc. Chem. Res.* **2004**, *37*, 854–861.
(10) Murgida, D. H.; Hildebrandt, P.; Wei, J.; He, Y.-F.; Liu, H.; Waldeck, D. H. *J. Phys. Chem. B* **2004**, *108*, 2261–2269.
(11) Song, S.; Clark, R. A.; Bowden, E. F.; Tarlov, M. J. *J. Phys. Chem.* **1993**, *97*, 6564–6572.
(12) Tarlov, M. J.; Bowden, F. F. *J. Am. Chem. Soc.* **1991**, *113*, 1847.

(13) Wei, J.; Liu, H.; Dick, A. R.; Yamamoto, H.; He, Y.; Waldeck, D. H. *J. Am. Chem. Soc.* **2002**, *124*, 9591–9599.
(14) Wei, J.; Liu, H.; Khoshtariya, D. E.; Dick, A.; Waldeck, D. H. *Angew. Chem., Int. Ed.* **2002**, *41*, 4700–4703.
(15) Wei, J. J.; Liu, H.; Niki, K.; Margoliash, E.; Waldeck, D. H. *J. Phys. Chem. B* **2004**, *108*, 16912–16917.
(16) Yue, H.; Khoshtariya, D.; Waldeck, D. H.; Grochol, J.; Hildebrandt, P.; Murgida, D. H. *J. Phys. Chem. B* **2006**, *110*, 19906–19913.
(17) Yue, H.; Waldeck, D. H.; Clark, R. A.; Petrovic, J. *J. Phys. Chem. B* **2006**, *110*, 5062–5072.
(18) Margoliash, E.; Schejeter, A. In *Cytochrome c: a Multidisciplinary Approach*; Scott, R. A.; Mauk, A. G., Eds.; University Science Books: Sausalito, CA, 1996.
(19) Collinson, M.; Bowden, E. F.; Tarlov, M. J. *Langmuir* **1992**, *8*, 1247–1250.
(20) Mauk, M. R.; Mauk, A. G. *Eur. J. Biochem.* **1989**, *186*, 473–483.
(21) Davis, K. L.; Drews, B. J.; Yue, H.; Knorr, K.; Clark, R. A.; Waldeck, D. H. *J. Phys. Chem. C.* **2008**, *112*, 6571–6576.
(22) Petrovic, J.; Clark, R. A.; Yue, H.; Waldeck, D. H.; Bowden, E. F. *Langmuir* **2005**, *21*, 6308–6316.
(23) Yue, H.; Waldeck, D. H.; Schrock, K.; Kirby, D.; Knorr, K.; Switzer, S.; Rosmus, J.; Clark, R. A. *J. Phys. Chem. B* **2007**, *xx*, xx–xx, accepted Oct.
(24) Xu, W.; Zhou, H.; Regnier, F. E. *Anal. Chem.* **2003**, *75*, 1931–1940.
(25) Chi, Q. J.; Zhang, J. D.; Andersen, J. E. T.; Ulstrup, J. *J. Phys. Chem. B* **2001**, *105*, 4669–4679.
(26) Fujita, K.; Nakamura, N.; Ohno, H.; Leigh, B. S.; Niki, K.; Gray, H. B.; Richards, J. H. *J. Am. Chem. Soc.* **2004**, *126*, 13954–13961.
(27) Smalley, J. F.; Feldberg, S. W.; Chidsey, C. E. D.; Linford, M. R.; Newton, M. D.; Liu, Y. P. *J. Phys. Chem.* **1995**, *99*, 13141–13149.
(28) Smalley, J. F.; Finklea, H. O.; Chidsey, C. E. D.; Linford, M. R.; Creager, S. E.; Ferraris, J. P.; Chalfant, K.; Zawodzinsk, T.; Feldberg, S. W.; Newton, M. D. *J. Am. Chem. Soc.* **2003**, *125*, 2004–2013.
(29) Smalley, J. F.; Sachs, S. B.; Chidsey, C. E. D.; Dudek, S. P.; Sikes, H. D.; Creager, S. E.; Yu, C. J.; Feldberg, S. W.; Newton, M. D. *J. Am. Chem. Soc.* **2004**, *126*, 14620–14630.
(30) Khoshtariya, D. E. D.; Tina, D.; Zusman, Leonid, D.; Waldeck, David, H. *J. Phys. Chem. A* **2001**, *105*, 1818–1829.
(31) Chidsey, C. E. D. *Science* **1991**, *252*, 919–922.
(32) Napper, A. M.; Liu, H.; Waldeck, D. H. *J. Phys. Chem. B* **2001**, *105*, 7699–7707.
(33) Bard, A. J.; Faulkner, L. R. *Electrochemical methods: fundamentals and applications*; 2nd ed.; John Wiley & Sons, Inc.: New York, 2001.
(34) Taylor, J. R. *An Introduction to Error Analysis*; 2nd ed.; University Science Books: Sausalito, CA, 1982.
(35) Zusman, L. D. *Chem. Phys.* **1987**, *112*, 53–59. Note that Zusman's result has an extra logarithmic term that arises from integration over the distribution of distances of the redox couples from the electrode surface. For the current case, the distance is taken to be fixed and the result simplifies to that given in eq 1.
(36) Zusman, L. D. *Z. Phys. Chem.—Int. J. Res. Phys. Chem. Chem. Phys.* **1994**, *186*, 1–29.
(37) Bertini, I.; Huber, J. G.; Luchinat, C.; Piccoli, M. *J. Magn. Reson.* **2000**, *147*, 1–8.
(38) Qi, P. X.; Urbauer, J. L.; Fuentes, E. J.; Leopold, M. F.; Wand, J. A. *Struct. Biol.* **1994**, *1*, 378–382.
(39) Xu, J.; Bowden, E. F. *J. Am. Chem. Soc.* **2006**, *128*, 6813–6822.
(40) Leopold, M. C.; Black, J. A.; Bowden, E. F. *Langmuir* **2002**, *18*, 978–980.
(41) Leopold, M. C.; Bowden, E. F. *Langmuir* **2002**, *18*, 2239–2245.
(42) Dolidze, T. D.; Rondinini, S.; Vertova, A.; Waldeck, D. H.; Khoshtariya, D. E. *Biopolymers* **2007**, *87*, 68–73.
(43) Yue, H.; Waldeck, D. H.; Schrock, K.; Kirby, D.; Knorr, K.; Switzer, S.; Rosmus, J.; Clark, R. A. *J. Phys. Chem. C* **2008**, *112*, 2514–2521.
(44) Pelletier, H.; Kraut, J. *Science* **1992**, *258*, 1748–1755.
(45) El Kasmi, A.; Wallace, J. M.; Bowden, E. F.; Binet, S. M.; Linderman, R. J. *J. Am. Chem. Soc.* **1998**, *120*, 225–226.
(46) Cukier, R. I. *J. Phys. Chem.* **1996**, *100*, 15428–15443.
(47) Cukier, R. I.; Nocera, D. G. *Annu. Rev. Phys. Chem.* **1998**, *49*, 337.
(48) Hammes-Schiffer, S. *Acc. Chem. Res.* **2001**, *34*, 273–281.
(49) Soudackov, A.; Hammes-Schiffer, S. *J. Chem. Phys.* **1999**, *111*, 4672–4687.
(50) Soudackov, A.; Hammes-Schiffer, S. *J. Chem. Phys.* **2000**, *113*, 2385–2396.
(51) Decornez, H.; Hammes-Schiffer, S. *J. Phys. Chem. A* **2000**, *104*, 9370–9384.
(52) Milne, J. S.; Mayne, L.; Roder, H.; Wand, J. A.; Englander, S. W. *Protein Sci.* **1998**, *7*, 739–745.
(53) Banci, L.; Bertini, I.; Gray, H. B.; Luchinat, C.; Reddig, T.; Rosato, A.; Turano, P. *Biochemistry* **1997**, *36*, 9867–9877.
(54) Banci, L.; Bertini, I.; Huber, J. G.; Spyroulia, G. A.; Turano, P. *J. Biol. Inorg. Chem.* **1999**, *4*, 21–31.
(55) Feng, Y.; Roder, H.; Englander, S. W. *Biochemistry* **1990**, *29*, 3494–3504.
(56) Berghuis, A. M.; Guillemette, J. G.; McLendon, G.; Sherman, F.; Smith, M.; Brayer, G. D. *J. Mol. Biol.* **1994**, *236*, 786–799.
(57) Glasoe, P. K.; Long, F. A. *J. Phys. Chem.* **1960**, *64*, 188–190.

JP803006B